Near-Threshold Electron-Impact Excitation of the Low-Lying Rydberg States of Ethylene

Daniel E. Love* and Kenneth D. Jordan

Department of Chemistry, University of Pittsburgh, Pittsburgh, PA 15260

Received: February 10, 1999; In Final Form: May 19, 1999

Excitation functions for the $^3B_{3u}$ $\pi \rightarrow$ 3s and $^3B_{1g}$ and ^1A_g $\pi \rightarrow$ 3p Rydberg states of ethylene have been measured and found to display structure due to the decay of core-excited anion states. Evidence is also provided that the $\pi^{-1}(3s)^2$ anion state undergoes significant decay to the $\pi \rightarrow \pi^*$ singlet state in highly twisted configurations.

1. Introduction

The electronic spectrum of the ethylene molecule has been the subject of numerous experimental[1−9] and theoretical[10−18] studies. Electron energy loss spectroscopy, since it permits characterization of dipole- and spin-forbidden transitions, has played a particularly important role in elucidating the excited states of ethylene.[2−6] In this context, it should be noted that there are two distinct mechanisms for the production of electronically excited states via electron impact: (1) direct excitation and (2) indirect excitation proceeding through the formation and decay of intermediate temporary anion states.[19] Most electron-energy-loss studies of the electronically excited states of ethylene have focused on direct excitation processes.

The present study examines the production of the electronically excited states of ethylene through the decay of temporary anion states. This includes exploring the possibility that the decay of temporary anion states can be used to probe normally inaccessible regions of the $^1B_{1u}$ $\pi \rightarrow \pi^*$ potential energy surface of the neutral molecule. For this to be a viable approach, it is necessary that the temporary anion state (assumed to be formed by vertical electron capture) undergo considerable nuclear distortion prior to electron detachment. Although measurements of vibrational excitation cross sections for electron impact provide ample evidence of the importance of geometrical distortions for valence-type temporary anion states,[20] the lifetimes of most valence-type temporary anion states are too short to permit sampling of regions of the potential energy surface far removed from that of the initial electron capture. On the other hand, Feshbach resonances, such as the $\pi^{-1}(3s)^2$ anion state of ethylene, tend to be relatively long-lived and, thus, are more attractive candidates for intermediates, leading to highly distorted structures of neutral molecules. Thus, the decay of Feshbach resonances via electron autodetachment would nicely compliment the more common use of bound anions, combined with electron photodetachment, for accessing neutral molecules at distorted geometries.[21−23]

2. Experimental Section

The magnetically collimated electron-energy-loss spectrometer used in this work has been described previously,[24,25] and only the salient features are covered here. The instrument employs three trochoidal monochromators[26] in a collinear geometry. A single monochromator is used to select the energy of the incident electrons (E_{in}) which are passed through a static cell where scattering with the target gas takes place, and a dual-stage monochromator is used to analyze the residual energy (E_{res}) of the scattered electrons. The electrons are counted at a dual-microchannel plate detector. The measured scattering cross sections are limited by the linear geometry of the instrument to the forward and backward directions, producing cross sections that are superpositions of the 0° and 180° partial cross sections.[24] The transmission efficiency of the analyzer is inversely proportional to the pass energy; to correct for this, each data point in the excitation functions has been multiplied by the analyzer energy at that point. This simple correction procedure has been found to be reliable in the energy range from threshold to 10 eV.[24] The incident energy was calibrated to the 6.66-eV $\pi^{-1}(3s)^2$ Feshbach resonance of ethylene,[27,28] and the energy loss was calibrated using the sharp Rydberg state at 8.26 eV.[2] The instrumental resolution was about 70 meV, and the calibration is expected to be accurate to ±35 meV.

3. Results and Discussion

Constant Residual Energy Spectra. Figure 1 displays electron-energy-loss spectra obtained with constant residual energies of 0.08, 0.13, 0.18, 0.31, and 0.41 eV. The spectra are plotted as a function of $E_{loss} = E_{in} - E_{res}$, where E_{in} and E_{res} are the incident and residual energies, respectively. The 1^3B_{1u} $\pi \rightarrow \pi^*$ state is visible near 4.2 eV in the $E_{res} = 0.08$ eV spectrum (which was the only one recorded below 5 eV). The $E_{res} = 0.08$ eV spectrum also displays a series of sharp peaks starting at $E_{loss} = 6.57$ eV. This structure moves to lower energy-loss values and diminishes in intensity as the residual energy is increased, indicating that it arises from a temporary anion state. The anion state involved is the lowest Feshbach resonance that has the $\pi^{-1}(3s)^2$ configuration and that has been observed previously in the $E_{loss} = 6.30$ and 6.66 eV excitation functions for the 1^1B_{1u} state (see Figure 2 and ref 29) as well as in electron transmission spectra (ETS), where it appears as a series of five peaks at 6.66, 6.83, 6.98, 7.16, and 7.32 eV,[27,28] due to the $\nu = 0-4$ members of the C=C stretch progression. The sharp structure observed in the present constant residual energy spectra has nearly the same spacings as that observed in the electron transmission spectrum for the $\pi^{-1}(3s)^2$ anion state, consistent with the interpretation that it arises from this species.

The low-energy vibrational levels of the $\pi^{-1}(3s)^2$ anion state can decay only to the ground state and the triplet and singlet π

* Present address: Division of Natural and Professional Sciences, Schreiner College, 2100 Memorial Blvd, Kerrville, TX 78028.

10.1021/jp990509k CCC: $18.00
Published on Web 07/02/1999

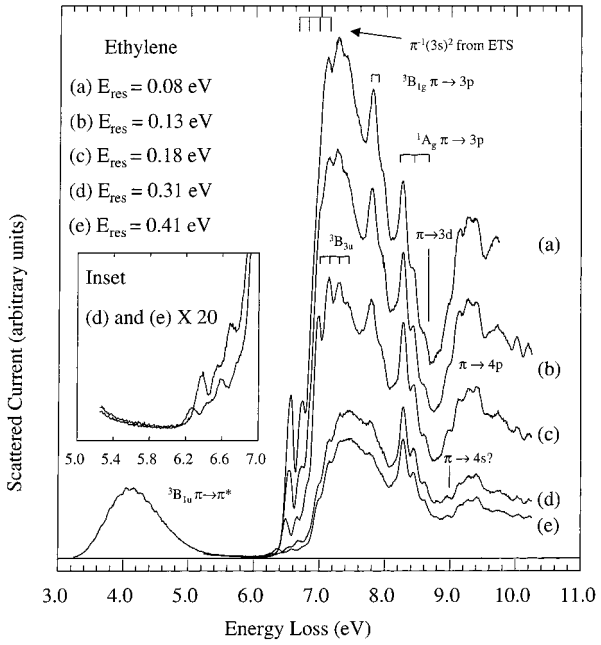

Figure 1. Energy-loss spectrum of ethylene obtained at constant residual energies of (a) 0.08, (b) 0.13, (c) 0.18, (d) 0.31, and (e) 0.41 eV. The inset shows the 5−7-eV region of the $E_{res} = 0.31$ and 0.41 eV spectra multiplied by 20. The assignments of the various electronically excited states are indicated. The positions of the $\nu = 0-3$ members of the C=C stretch progression in the $\pi^{-1}(3s)^2$ anion state (as observed in ETS) are indicated at the top of the figure.

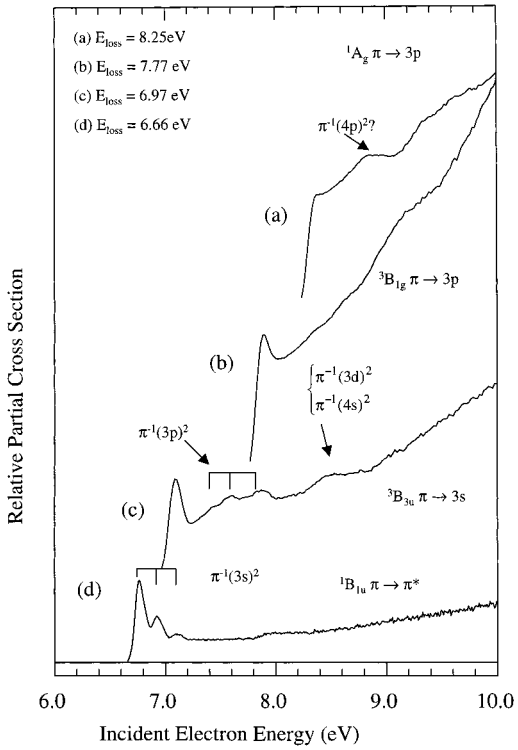

Figure 2. Relative partial cross sections for excitation of the ^1A_g and $^3B_{1g}\pi \rightarrow 3p$, $^3B_{3u}\ \pi \rightarrow 3s$, and $^1B_{1u}\ \pi \rightarrow \pi^*$ states of ethylene at energy-loss values of (a) 8.25, (b) 7.77, (c) 6.97, and (d) 6.66 eV, respectively. Structures arising from the $\pi^{-1}(3s)^2$, $\pi^{-1}(3p)^2/\pi^{-1}(4s)^2$, and $\pi^{-1}(4p)^2$ anion states are indicated.

$\rightarrow \pi^*$ states of the neutral molecule (as these are the only energetically accessible states). The appearance of the sharp structure at low energies in the constant residual energy spectra strongly suggests that part of the decay is to the singlet $\pi \rightarrow \pi^*$ state. The lowest energy feature observed in the $E_{res} = 0.41$ eV spectrum falls at 6.25 eV, 0.6−0.8 eV above the origin[6,8] of the singlet $\pi \rightarrow \pi^*$ state, which has a perpendicular D_{2d} equilibrium structure.[13,15,30,31]

In the $\pi^{-1}(3s)^2$ region of the constant residual energy spectra, the second and fourth peaks are weaker than the first and third peaks; this is especially apparent in the $E_{res} = 0.31$ and 0.41 eV spectra shown in the inset. This alternating intensity pattern is not observed in the electron transmission spectrum. This could be the consequence of the different decay channels "sampled" in the two experiments: The energy-loss spectra necessarily represent inelastic decay processes, whereas ETS is dominated by the elastic channel. Specifically, the alternating intensity pattern in the constant residual energy spectra could be due to the decay of the $\pi^{-1}(3s)^2$ anion state to the singlet $\pi \rightarrow \pi^*$ state. The electron transmission spectra reveal that the torsional mode is excited upon electron capture to form the $\pi^{-1}(3s)^2$ state, and it is possible that this mode is involved in the decay to the singlet $\pi \rightarrow \pi^*$ state.

The $\pi^{-1}(3s)^2$ anion state, like its parent Rydberg state, is expected to be twisted about 25° from planar.[32] The decay of the $\pi^{-1}(3s)^2$ anion state to the $\pi \rightarrow \pi^*$ excited state requires configuration mixing in one or both states. (Mixing between the $\pi^{-1}(3s)^2$ and $\pi^{-1}(\pi^*)^2$ anionic configurations seems especially likely.) In the region of the $\pi \rightarrow 3s$ states (7.0−7.5 eV), the shape and relative intensities of the peaks in the spectra change considerably as the residual energy is increased from 0.08 to 0.31 eV. In contrast, the $E_{res} = 0.31$ and 0.41 eV spectra are nearly indentical. Although vibrational structure due to the $1^3B_{3u}\ \pi \rightarrow 3s$ state might be expected in the $E_{res} = 0.08$ and 0.13 eV spectra, it is obscured by the structure due to the decay of the $\pi^{-1}(3s)^2$ anion state to the underlying $^1B_{1u}\ \pi \rightarrow \pi^*$ state. Of the spectra reported in Figure 1, the vibrational structure in the 7.0−7.5-eV region is sharpest in the $E_{res} = 0.18$ eV spectrum, with pronounced peaks visible at 6.98, 7.13, and 7.29 eV, followed by a weaker peak at 7.42 eV. This structure is believed to derive mainly from the $1^3B_{3u}\ \pi \rightarrow 3s$ state.[5]

At somewhat higher energies, the $E_{res} = 0.08-0.41$ eV spectra display peaks at 7.78 and 8.26 eV and weaker features near 7.93, 8.42, and 8.60 eV. The peak at 7.78 eV is quite strong in the $E_{res} = 0.08$ eV spectrum, but the intensities of this feature and of the accompanying 7.93-eV shoulder decrease rapidly as the residual energy is increased. This is consistent with this structure being due to the $^3B_{1g}\ \pi \rightarrow 3p_y$ state as assigned in ref 5. The 7.93-eV shoulder is likely due to one quantum of C=C stretch in the $^3B_{1g}$ state, although it may also result, in part, from the $^1B_{2g}$ or $^3B_{2g}\ \pi \rightarrow 3p_z$ states. (MPI measurements place the $^1B_{1g}$ state at 7.90 eV.[7,9]) Reference 5 reported a feature at 8.15 eV that was assigned to the $^3A_g\ \pi \rightarrow 3p_x$ state; however, our spectra do not show a feature at this energy. The strong peak observed near 8.26 eV and the shoulder at 8.42 eV retain appreciable intensity as the residual energy is increased from 0.08 to 0.41 eV. This structure is attributed to the $^1A_g\ \pi \rightarrow 3p_x$ state reported previously at 8.29 eV.[7,9] The weak feature at 8.60 eV is assigned to one or more of the $\pi \rightarrow 3d_\sigma$ states that have been observed at 8.62 eV.[5,33]

The constant residual energy spectra also display considerable structure above 8.8 eV. For example, the $E_{res} = 0.31$ eV spectrum has peaks at 8.95, 9.14, 9.28, and 9.39 eV, for which there are no corresponding features of comparable intensity in the optical spectrum. The CIS calculations of Wiberg et al.[14] place the three $\pi \rightarrow 4p$ states at 9.09, 9.19, and 9.29 eV. This suggests that the 9.14-, 9.28-, and 9.39-eV features in the present spectra are due to the three $\pi \rightarrow 4p$ states and that the 8.95-eV

feature is due to a $\pi \rightarrow$ 4s state, although we cannot rule out an alternative interpretation that all the structure between 8.9 and 9.4 eV is due to $\pi \rightarrow$ 4p states, with one or more of the peaks being due to the vibrational structure. The energy-loss spectra of Wilden et al.[5] displayed two peaks at 9.36 and 9.50 eV, which were tentatively identified as the three $\pi \rightarrow$ 4p states. The 9.36-eV feature of Wilden et al. almost certainly corresponds to that observed at 9.39 eV in our spectra and that we believe is the highest energy $\pi \rightarrow$ 4p state. If this interpretation is correct, the 9.50-eV feature observed by Wilden et al. could then correspond to a vibrationally excited level of this state. Our energy-loss spectra also display peaks near 9.7, 10.0, and 10.3 eV, which could be due to $\pi \rightarrow$ 5p Rydberg transitions.

Constant Energy-Loss Spectra. Figure 2 displays the spectra obtained with fixed energy-loss values of 6.97, 7.77, and 8.25 eV, which correspond to excitation of the $\nu = 0$ levels of the $^3B_{3u}$ $\pi \rightarrow$ 3s, $^3B_{1g}$ $\pi \rightarrow$ 3p, and ^1A_g $\pi \rightarrow$ 3p Rydberg states, respectively. At higher energies, each of these excitation functions increases nearly linearly with increasing incident energy, which reflects some contribution from the underlying $^1B_{1u}$ $\pi \rightarrow \pi^*$ transition. The $E_{loss} = 6.66$ eV [$^1B_{1u}$ $\pi \rightarrow \pi^*$] excitation function, for which decay to the Rydberg states is not possible energetically, is included for comparison. This excitation function displays a series of sharp features at 6.77, 6.92, and 7.10 eV that correspond to the $\nu = 1$, 2, and 3 levels of the C=C stretch progression in the $\pi^{-1}(3s)^2$ anion. Each of these three peaks lies 0.06 eV lower than the corresponding level in the electron transmission spectrum. Although part of this energy difference could be "nonphysical" (e.g., due to errors in calibration), part of the offset could be "physical" in the sense that the structure due to temporary anions can appear at different energies in different decay channels.[19] The electron transmission experiment is a total cross-section measurement which is expected to be dominated by the elastic scattering component, whereas the structure in the excitation function results from inelastic processes, with the dominant channel believed to be decay to the singlet $\pi \rightarrow \pi^*$ state.[29]

The $E_{loss} = 6.97$ eV spectrum displays a sharp peak at 7.10 eV that is attributed to the $\nu = 3$ level of the $\pi^{-1}(3s)^2$ anion. Energetically, the $\nu = 3$ level of the anion can decay to the $\nu = 0$ (C=C stretch) level of its parent $^3B_{3u}$ $\pi \rightarrow$ 3s state. However, since the $\pi \rightarrow$ 3s Rydberg and $\pi^{-1}(3s)^2$ anion states should have very similar potential energy surfaces, the Franck–Condon overlap for this decay process should be very small. Therefore, we believe that the 7.10-eV peak in the $E_{loss} = 6.97$ eV spectrum is almost entirely the result of decay of the $\nu = 3$ (C=C stretch) level of the $\pi^{-1}(3s)^2$ anion to the underlying $^1B_{1u}$ $\pi \rightarrow \pi^*$ state.

Each of the four fixed energy-loss spectra shown in Figure 2 displays structure at incident energies above 7.4 eV. The $E_{loss} = 6.66$ eV spectrum displays a weak broad feature extending from 7.8 to 8.3 eV. The $E_{loss} = 6.97$ eV spectrum displays features at 7.40, 7.60, 7.80, and 8.5 eV. The first three of these features are assigned to Feshbach resonances with $\pi^{-1}(3p)^2$ configurations; the higher energy feature is expected to be due to a $\pi^{-1}(3d)^2$ or a $\pi^{-1}(4s)^2$ anion state. The latter assignment is based on the observation of the $\pi \rightarrow 3d_\sigma$ and $\pi \rightarrow$ 4s states of the neutral molecule at 8.62[5,33] and 8.90 eV,[5] respectively, and the fact that Feshbach resonances generally lie a few tenths of an electronvolt lower in energy than their parent Rydberg states.[19] Decay of $\pi \rightarrow 3d_\sigma$ anion states to the triplet $\pi \rightarrow$ 3s Rydberg state would be facilitated by configuration mixing. The $E_{loss} = 7.77$ eV spectrum has a sharp peak near 7.90 eV that is apparently due to the $\pi^{-1}(3p)^2$ anion state observed at 7.80 eV in the $E_{loss} = 6.97$ eV spectrum. The $E_{loss} = 7.77$ eV spectrum also displays very weak structure at 8.4 and 8.6 eV, which is probably of the same origin as the broad feature centered at 8.5 eV in the $E_{loss} = 6.97$ eV spectrum. The $E_{loss} = 8.25$ eV spectrum does not display a peak near the threshold but does display a broad peak near 8.8 eV, which is likely due to $\pi^{-1}(4p)^2$ anion states.

4. Conclusions

Near-threshold electron-energy-loss spectra, for energy losses up to about 10 eV, have been obtained for ethylene. The constant residual energy spectra reveal sharp structure due to the formation and decay of the $\pi^{-1}(3s)^2$ Feshbach resonance. Part of the decay is to the underlying $^1B_{1u}$ $\pi \rightarrow \pi^*$ state. The energy of the vibrational zero-point level of the $^1B_{1u}$ $\pi \rightarrow \pi^*$ state has been estimated to lie between 5.4 and 5.7 eV,[6,8,15,16,31] about 2 eV below the vertical excitation energy (7.7 eV). With a E_{res} value of 0.41 eV, the largest used in this study, the singlet $\pi \rightarrow \pi^*$ state can be formed at 6.25 eV upon decay of the 6.66-eV $\pi^{-1}(3s)^2$ anion state. Given the magnitudes of the structure in the $E_{res} = 0.41$ eV spectrum, it seems highly probable that with use of larger residual energies, it would be possible to access even lower energy vibrational levels (and, perhaps, even the origin) of the $^1B_{1u}$ $\pi \rightarrow \pi^*$ state by this decay mechanism.

The electron-energy-loss spectra also show structure assigned to the $^3B_{3u}$ $\pi \rightarrow$ 3s state (6.97 eV) and the $^3B_{1g}$ and ^1A_g $\pi \rightarrow$ 3p Rydberg states at 7.77 and 8.25 eV, respectively. In addition, structure attributed to $\pi \rightarrow$ 4p Rydberg states is observed between 9.1 and 9.4 eV.

The excitation functions for the $^1B_{1u}$ $\pi \rightarrow \pi^*$, $^3B_{3u}$ $\pi \rightarrow$ 3s, $^3B_{1g}$ $\pi \rightarrow 3p_y$, and ^1A_g $\pi \rightarrow 3p_x$ states were obtained by scanning the incident energy with fixed energy losses of 6.66, 6.97, 7.77, and 8.25 eV, respectively. Both the $E_{loss} = 6.66$ and 6.97 eV spectra display sharp structure due to the formation of the $\pi^{-1}(3s)^2$ anion and its subsequent decay to the underlying $^1B_{1u}$ $\pi \rightarrow \pi^*$ state and higher lying Feshbach resonances.

Acknowledgment. This research was supported by a grant from the National Science Foundation.

References and Notes

(1) Wilkinson, P. G.; Mulliken, R. S. *J. Chem. Phys*. **1995**, *23*, 1895.
(2) Wilden, D. G.; Comer, J. *J. Chem. Phys*. **1980**, *13*, 1009.
(3) Van Veen, E. H. *Chem. Phys. Lett*. **1976**, *41*, 540.
(4) Verhaart, G. J.; Brongersma, H. H. *Chem. Phys. Lett*. **1980**, *71*, 345.
(5) Wilden, D. G.; Comer, J. *J. Phys. B* **1980**, *13*, 1009.
(6) McDiarmid, R. *J. Chem. Phys*. **1977**, *67*, 3835.
(7) Gedanken, A.; Kuebler, N. A.; Robin, M. B. *J. Chem. Phys*. **1982**, *76*, 46.
(8) Robin, M. B. *Higher Excited States of Polyatomic Molecules*; Academic Press: New York, 1985; Vol. III and references therein.
(9) Williams, B. A.; Cool, T. A. *J. Chem. Phys*. **1991**, *94*, 6358.
(10) Serrano-Andres, L.; Merchan, M.; Nebot-Gill, I.; Lindh, R.; Roos, B. O. *J. Chem. Phys*. **1993**, *98*, 3151.
(11) Krebs, S.; Buenker, R. J. *J. Chem. Phys*. **1997**, *106*, 7208.
(12) Peyerimhoff, S. D.; Buenker, R. J. *Theoret. Chim. Acta*. **1972**, *27*, 243.
(13) Petrongolo, C.; Buenker, R. J.; Peyerimhoff, S. D. *J. Chem. Phys*. **1982**, *76*, 3655.
(14) Wiberg, K. B.; Hadad, C. M.; Foresman, J. B.; Chupka, W. A. *J. Phys. Chem*. **1992**, *96*, 10756.
(15) Mebel, A. M.; Chen, Y.; Lin, S. *J. Chem. Phys*. **1996**, *105*, 9007.
(16) Mebel, A. M.; Chen, Y.; Lin, S. *Chem Phys. Lett*. **1996**, *258*, 53.
(17) Mebel, A. M.; Hayashi, M.; Lin, S. *Chem Phys. Lett*. **1997**, *274*, 53.
(18) Ryu, J.; Hudson, B. S. *Chem. Phys. Lett*. **1995**, *245*, 448.
(19) Schulz, G. J. *Rev. Mod. Phys*. **1973**, *45*, 378.
(20) Allan, M. *Chem. Phys*. **1984**, *86*, 303.
(21) Neumark, D. M. *Science* **1996**, *272*, 5267.

(22) Neumark, D. M. *Science* **1993**, *262*, 5141.
(23) de Beer, E.; Kim, E. H.; Neumark, D. M.; Gunion, R. F.; Lineberger, W. C. *J. Phys. Chem*. **1995**, *99*, 13627.
(24) Allan, M. *J. Elec. Spectrosc. Rel. Phenom.* **1989**, *48*, 219.
(25) Falcetta, M. F.; Jordan, K. D. *J. Am. Chem. Soc*. **1991**, *113*, 7455.
(26) Stamatovic, A.; Schulz, G. J. *Rev. Sci. Instrum*. **1970**, *41*, 423.
(27) Jordan, K. D.; Burrow, P. D. *ACS Symp. Ser*. **1984**, *263*, 165.
(28) Sanche, L.; Schulz, G. J. *J. Chem. Phys*. **1973**, *58*, 479.
(29) Love, D. E.; Jordan, K. D. *Chem. Phys. Lett*. **1995**, *235*, 479.
(30) Sension, R. J.; Hudson, B. S. *J. Chem. Phys*. **1989**, *90*, 1377.
(31) Dauber, P.; Brith, M.; Huler, E.; Warshel, A. *Chem. Phys*. **1975**, *7*, 108.
(32) Merer, A. J.; Schoonveld, L. *Can. J. Phys*. **1969**, *47*, 1731.
(33) McDiarmid, R. *J. Phys. Chem*. **1980**, *84*, 64.